

Chapter 11

Rational Design of Graphene-based Sorbents for Water Purification



Asif Hussain, Muhammad Usman, Rana Zafar Abbas Manj, Fuqiang Liu, Dengxin Li, and Yanbiao Liu

11.1 Introduction

The textile industry, one of the major industries of China, plays a pivotal role in boosting the economic development [1, 2]. Meanwhile, it also causes serious environmental pollution due to discharge of excess dyes into water bodies. The textile industry has been listed by the Chinese government as the key industry that needs to be rectified and improved. However, the textile wastewater is usually characterized by complex compositions, large volume, poor biodegradability, and high chrominance which render it one of the hardest-to-treat forms of industrial wastewater [2, 3]. Therefore, it is highly desirable to develop advanced approaches to address this challenging issue [4]. Different processes have been developed and applied for the treatment of textile wastewater. For example, conventional biological processes demonstrated limited capability for dye degradation due to their poor biodegradability [5]. Chemical oxidation methods like photocatalytic oxidation [6] and ozonation [7] are usually energy intensive and expensive, while catalytic oxidation based on peroxymonosulfate activation may lead to the generation of insufficient

A. Hussain

College of Environmental Science and Engineering, Donghua University, Shanghai, China

Department of Environmental Science, Federal Urdu University of Arts, Science and Technology, Karachi, Pakistan

M. Usman

PEIE Research Chair for the Development of Industrial Estates and Free Zones, Center for Environmental Studies and Research, Sultan Qaboos University, Al Khoudh, Muscat, Oman

R. Z. A. Manj

College of Material Science and Engineering, Donghua University, Shanghai, China

F. Liu · D. Li · Y. Liu (✉)

College of Environmental Science and Engineering, Donghua University, Shanghai, China

e-mail: yanbiaoliu@dhu.edu.cn

mineralization or byproducts, causing further secondary pollution [8]. Dye rejection by state-of-the-art membrane processes is feasible; however, the high turbidity and complex compositions of the dye wastewater can easily block membrane pores and decrease membrane efficacy [9]. Alternatively, adsorption has received significant interest from the scientific community to serve as a promising, affordable, and viable technology to remove dyes from water [10, 11].

Carbon-based materials have been extensively investigated due to their intriguing physicochemical properties [11, 12]. Among them, graphene compounds have been extensively studied for various environmental applications [9, 12, 13]. In this chapter, we summarized the recent advances on the rational design of graphene-based sorbents. Their applications in dye removal are introduced in detail in terms of sorption kinetics and thermodynamics. At last, existing challenges and future prospects are provided.

11.2 Overview of Graphene-based Sorbents

11.2.1 Graphene Oxide Adsorbents

Graphite oxide (GO) is an important derivative of graphene in highly oxidized form (i.e., containing oxo functionalities and hydrogen atoms) [15]. It is usually synthesized through chemical oxidation of pristine graphite followed by exfoliation [16]. The exact chemical structure and composition of GO are still debatable due to the complexity and variability of GO samples arising from different synthesis conditions and non-stoichiometric atomic compositions of $C_xH_yO_z$ [17]. Many chemical structural models have been proposed for GO (e.g., Hofmann model [18], Ruess model [19], Scholz–Boehm model [20], Nakajima–Matsuo model [21], Lerf–Klinowski model [22, 23], or Szabo model [24]). They show mostly a layered structure of graphite with diverse oxygen functionalities [14, 25]. Among these models, Lerf–Klinowski model is the most acceptable [26], in which the characteristic GO functional defect sites are decorated with carbonyl, epoxy, carboxyl, and hydroxyl groups [14, 26, 27]. The oxidation of graphite breaks the π – π conjugation of graphite flakes into nanoscale fragments of ordered- sp^2 graphitic domains (C=C) surrounded by disordered- sp^3 (C-C) oxidized domains [28]. The relative size of these domains depends on the oxidation degree of mother compounds [23]. The carbon-to-oxygen ratio (C/O) in GO usually varies from 1.5 to 2.5. The functional defect sites make GO highly hydrophilic to form a stable light brown suspension of single or multilayers GO sheets with an average dimension of 0.22 to ≥ 2.5 μm in water, depending on gradient differential centrifugation, GDC (Fig. 11.1) [14], and allow one to control the assembly behavior of macroscopic graphene [27].

The planar sp^2 aromatic domains and sp^3 hybridized edge sites make this nanomaterial amphiphilic or behave like a polymer for various covalent or noncovalent bonding interactions [29]. It should be noted that some dye molecules also contain

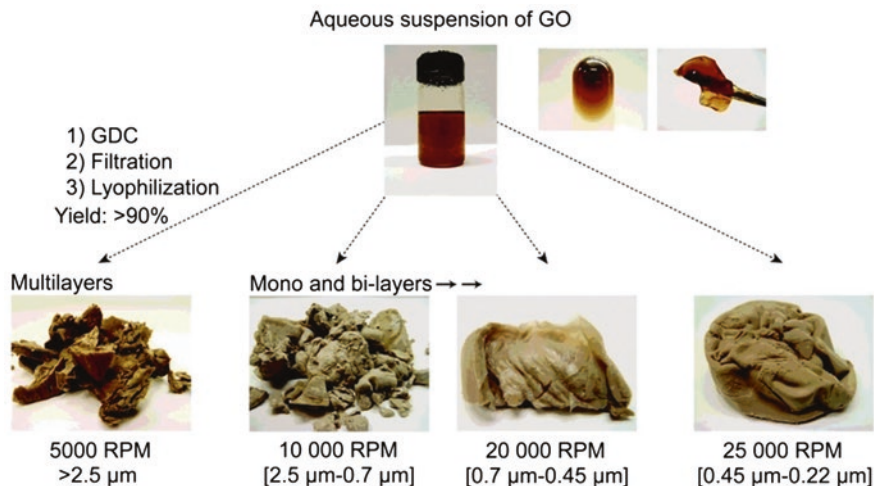


Fig. 11.1 Several fractions of GO aqueous suspensions after GDC and membrane filtration. Reproduced with permission [14]. Copyright 2020, Royal Society of Chemistry

aromatic structures, and exist usually in ionic form in water. GO is characterized by negatively charged surface over a wide pH range, which promotes an increased adsorption of the cationic dye methylene blue (MB) via electrostatic interaction [30]. GO has a larger and smoother surface than CNTs and activated carbon [31], which favors an additional contribution of π - π electron donor/acceptor interactions and causes an elevated adsorption capacity.

GO-based adsorbents can be prepared via Hummer's method with variable oxidation degree by using different oxidant doses (e.g., KMnO_4) and reaction conditions [32]. A quantitative measurement of GO oxidation degree has been performed using a combination of X-ray photon spectroscopy (XPS) and X-ray diffraction (XRD) to test for the MB removal. It was proposed that an improvement in oxidation degree can result in a strong affinity to MB due to alteration in the fundamental adsorption behavior of GO. For example, with an increase in the oxidation degree, the MB uptake capacity by GO can be increased exponentially [32]. It may change the isotherm adsorption behavior from Freundlich type to Langmuir type due to the generation of more active adsorption sites on the GO surface [32]. Furthermore, the relative proportion of these two functional regions in GO (e.g., oxidized GO-type, and non-oxidized graphite regions) was flexible to the oxidative conditions [32]. The binding features in the non-oxidative region of planar graphite tend to form parallel π - π stacking/hydrophobic interactions with MB molecules in water. In contrast, oxidized regions containing oxygen functionalities can bind these MB molecules vertically on the GO plane via electrostatic interactions or hydrogen bonding. It was proposed that the latter interaction mode usually exhibits stronger affinity toward cationic MB dye at higher oxidation degree. Furthermore, the adsorption of two anionic azo dyes (acid orange 8, AO8, and direct red 23, DR23) onto GO was

also investigated [33]. The adsorption data fitted well with the Langmuir isotherm with a maximum monolayer adsorption capacity of 29 ± 0.2 and 15 ± 0.3 mg/g for AO8 and DR23, respectively. The adsorption process of AO8 was exothermic, while the adsorption of DR23 was endothermic in nature. Adsorption of both dyes onto GO mainly occurred through electrostatic interaction, but hydrogen bonding and π - π stacking interactions were also involved [33].

Several studies suggested that a nanoscale GO adsorbent possesses a better potential for water purification compared to other carbon counterparts [30]. However, GO usually shows limited affinity to the anionic dyes due to strong electrostatic repulsion [34]. Further engineering concerns associated with the applications of nanoscale GO in powder forms are expensive recovery and/or reuse, and negative impacts on living organisms that seriously restrict its feasibility at industrial scale [35]. Consequently, the true revolutionary potential lies in diverse pathways for the tailored manipulation of graphene surface chemistry and can only be rationalized via bottom-up design synthesis.

11.2.2 Graphene Adsorbents

Reduced GO (rGO) or graphene is a two-dimensional carbon nanomaterial comprising a single layer of sp^2 carbon atoms arranged in a hexagonal ring [36]. rGO has attracted significant worldwide attention due to its outstanding physical, chemical, electrical, and mechanical properties [37]. The key opportunity to employ graphene as an adsorbent material is due to its high surface area up to 2630 g/m^2 [38] and high hydrophobicity (i.e., highly ordered- sp^2 graphitic domains) [17]. rGO can be prepared through wet chemistry reduction using a GO precursor and appropriate reducing agents (e.g., hydrazine [34], sodium ascorbate [39], hypophosphorous acid [40], ascorbic acid [41], urea [35], or thiourea [38]). It appears that each method produces graphene with different physicochemical characteristics (i.e., functionalities or degree of reduction), thereby showing different performances.

To boost their sorption performance, three-dimensional (3D) rGO hydrogels were developed via chemical approaches [39]. It was proposed that graphene nanosheets can be self-organized into a 3D porous network through *van der Waals* and π - π interactions [39]. As-obtained 3D mesoporous material showed maximum adsorption capacities of 8 ± 0.2 mg/g for MB and 29 ± 0.5 mg/g for RhB based on a heterogeneous type Freundlich isotherm model. The strong π - π stacking and anion-cation interactions were proposed to dictate the adsorption process. Sorbent recycling experiments showed that the materials could easily be regenerated by washing with ethylene glycol [39]. Furthermore, 3D microstructures of rGO were explored, which were prepared by heating the GO suspension in a mixture of hypophosphorous acid (H_3PO_2) and iodine (I_2) at 80°C for 12 h followed by freeze-drying [40]. The 3D-rGO macrostructures were examined to remove anionic acid red 1 (AC1) and cationic MB dyes. The surface charge of the 3D-rGO and the

chemical structure of the dye molecules caused notable differences in the overall adsorption capacity, equilibrium time, and adsorption mechanism [40]. The equilibrium data were best fitted to a Langmuir and Freundlich model for MB and AC1, respectively. This chemically reduced 3D-rGO provides an ideal platform for a fast adsorption of MB with a capacity of 300 mg/g. The electrostatic and π - π interactions between the localized π -electrons of conjugated aromatic rings in rGO and dye molecules were involved in the MB adsorption. However, the as-prepared 3D-rGO sorbent was unsuitable for the uptake of negatively charged AC1 (adsorption capacity of 277 mg/g) due to dissociated SO_3^- groups in aqueous solution [40].

Most of these reported designs existed in powder form [32–34, 37, 39, 40], which tend to generate irreversible agglomerates due to strong π - π stacking and *van der Waals* interaction between the graphene sheets. This seriously decreases the surface area. Alternatively, functional composites of graphene were modified further with magnetic nanoparticles [42, 43] or by coating onto different macroscopic supports [44, 45]. However, magnetic adsorbent designs frequently showed limited adsorption capability, resulting from reduced surface area due to large aspect ratio of graphene. Loss of active adsorbent sites during cross-linking or coating of graphene on other material may also be responsible for the reduced adsorption performance. Thus, other innovative and advanced designs to enhance the functionality of graphene adsorbents should be given an imperative focus.

11.3 Graphene-based Macroscopic Sorbents

The synthesis of 3D macroscopic structures is of importance toward the practical applications of graphene-based sorbents. Until now, template-directed [46–49] and template-free (i.e., self-assembled) methods [50–57] are two main routes for the integration of graphene nanosheets into a 3D macroscopic network. These 3D designs not only promote the exposure of adsorption active sites and facile transmission of pollutant molecules [58], but also allow affordable recycling potential and further modifications. For example, a random arrangement of GO sheets into a 3D network can create a sufficient porosity or out-of-plane space in-between graphene sheets, which decreases the π - π stacking between graphene nanosheets [58] and increases the exposure of adsorptive active sites for organic molecules. The macroscopic dimensions with hierarchical porous network (i.e., micro-, meso-, and macropores) can promote facile diffusion of pollutant molecules and allow simple and affordable reuse [59–61]. Furthermore, such designs can also host various functional guests (e.g., metals oxide, polymers, carbon nanofibers, CNTs, etc.) via covalent or noncovalent interactions, which result in the synergy of hierarchical structures and multifunctional properties for desired applications [35, 62, 63]. To date, an increasing number of macroscopic designs of graphene have been reported toward environmental remediation applications [36].

11.3.1 Template-Directed Design of Graphene Adsorbents

The template-directed macroscopic design of graphene can be prepared by hard [46] or soft-template [47–49, 64] methods using GO solution. Recent advances in the template-directed macroscopic designs of graphene adsorbents are listed in Table 11.1. A GO sponge, synthesized by a centrifugal vacuum and evaporation method, showed good removal performance of cationic dyes (MB and methyl violet, MV) from water (Fig. 11.2) with a fast equilibrium time of 2 min and adsorption capacities of 397 and 467 mg/g for MB and MV, respectively [47]. An endothermic type chemical adsorption of MB and MV on GO sponge was proposed through strong π - π stacking and anion-cation interactions with activation energies of 50 ± 0.3 and 71 ± 0.2 kJ/mol, respectively. However, extra post-filtration and insufficient reusability, due to inevitable re-dissolution of nanoscale GO after dye treatment, limit its water phase application.

Further, GO foam with macroporous architecture was prepared by direct lyophilization of GO dispersions [48]. The GO foam was tested to remove cationic dyes such as RhB, MG, and acriflavine (AF) containing different functional groups (e.g., xanthene fluorine rhodamine, tri-aryl methane, and acridine, respectively), but with similar molecular size. The adsorption capacities of GO foam were in the order of 446 mg/g (RhB) > 321 mg/g (MG) > 228 mg/g (AF). The electrostatic interactions between the GO foam and the dye molecules were proposed based on the recorded shifts of G-band toward lower wavenumbers in the Raman spectra. Furthermore, GO aerogel foams were prepared by a unidirectional ice segregation induced self-assembly method, in which a cylindrical plastic tube containing water suspension of GO (4 mg/mL) is placed into a Styrofoam container to provide a uniaxial thermal

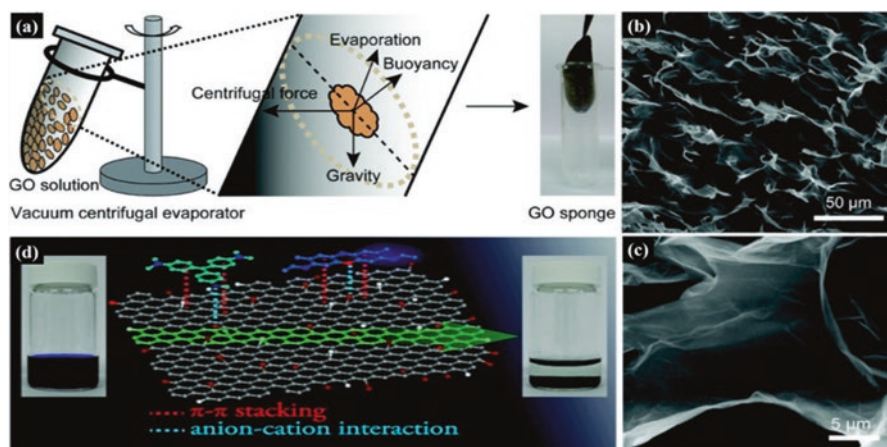


Fig. 11.2 Scheme for a physically cross-linked 3D GO sponge using a vacuum centrifugal evaporator method (a), SEM image in low magnification (b), high magnification of GO sponge (c), and dye adsorption mechanism (d) using GO sponge. Reproduced with permission from [47]. Copyright 2012, American Chemical Society

Table 11.1 Template-directed design of graphene sorbents to remove organic pollutants from water

Adsorbent	Synthesis protocol	Major additives	Pollutant	Q (mg/g)	References
GO foam	Centrifugal & vacuum evaporation	Additive free	MB	397	[47]
GO foam	Centrifugal & vacuum evaporation	Additive free	MV	467	[47]
GO foam	Ice template and freeze dry	Additive free	RhB	446	[48]
GO foam	Ice template and freeze dry	Additive free	MG	321	[48]
GO foam	Ice template and freeze dry	Additive free	AF	228	[48]
GO foam	Unidirectional ice segregation	Additive free	MB	416.67	[49]
rGO-LD sponge	Ice template and annealing	Laundry detergent	Diesel	–	[64]
rGO-SDS sponge	Ice template and annealing	SDS	Diesel	–	[64]
GO-PVA foams	Ice template & solvent exchange	PVA	MB	571.4	[65]
rGO-PVA foam	Ice template & solvent exchange	Ammonia / glucose	MB	81.0	[65]
GO-SA aerogel	Ice template & solvent exchange	Sodium alginate	MB	833.3	[25]
rGO-SA aerogel	Ice template & thermal reduction	Ammonia / glucose	MB	192.3	[25]
GO-agar aerogel	Ice template and freeze dry	Biopolymer agar	MB	476.8	[66]
GO-ECNFs aerogel	Ice template and freeze dry	ECNF	CV	>800	[67]
GO-ECNFs aerogel	Ice template and freeze dry	ESCNFs	MG	>800	[67]
GO-ESCNFs aerogel	Ice template and freeze dry	ESCNFs	RhB	>800	[67]
GO-PAA aerogels	Ice template and vacuum dry	PAA as cross-linker	Oil	120 g/g	[68]
GO-cellulose aerogel	Bidirectional freeze dry	Cellulose and saline	Oil	197 times	[69]
rGO-CNTs monolith	CVD method	CNTs	Oil	–	[70]
3D-rGO-Fe ₃ O ₄ aerogel	Polymer template & calcination	PMMA and Fe ₃ O ₄	MB	170.1	[46]
rGO-Cys monolith	3D printing	L-cysteine	IC	1005.7	[71]
rGO-Cys monolith	3D printing	L-cysteine	NR	1301.8	[71]

gradient using liquid N₂ [49, 72]. Next, the frozen suspension is freeze-dried to sublimate ice crystals and to obtain a GO aerogel, which is used to remove MB from water. The GO aerogel showed aligned porosity in the micrometer range, which allows the creation of an increased number of adsorption sites. A maximum adsorption capacity of 417 ± 0.5 mg/g was achieved based on the Langmuir isotherm model, while the adsorption process was suggested to be spontaneous and endothermic in nature.

Graphene sponge with a hierarchical porous network was developed using laundry detergent bubbles (B-LN) as a soft template by freezing rapidly in liquid N₂ and a subsequent annealing at 300 °C in Ar environment [64]. The formation mechanism involved the self-assembly of GO sheets copying the morphologies of original liquid-filled detergent bubbles. The structure can be tuned by changing the freezing media, adjusting the stirring rate, or adding functional additives. However, pure GO foams or aerogels prepared by a hard ice or a soft soap template method generally show weak and delicate 3D networks, which complicate their handling and limit their commercial implementation. Alternatively, various kinds of chemical additives (e.g., polyvinyl alcohol (PVA), sodium alginate (SA), agar, cellulose, chitosan, or CNTs) were employed to design mechanically stable GO foams via the template-directed methods.

For example, a macroporous composite foam of GO-PVA was synthesized through a process involving aqueous precursor solution freezing, solvent exchange (in ethanol), and drying [65]. The presence of frozen ice crystals created a porous structure of randomly oriented GO sheets surrounded by PVA. The yellow GO-PVA foam was reduced further by heating at 95 °C for 1 h with a tannery mixture of water/ammonia/glucose to obtain a black-colored rGO-PVA foam. GO-PVA and rGO-PVA monolithic foams were tested for the removal of soybean oil, ethanol, or the cationic MB dye from water. GO-PVA showed higher MB adsorption capacity of 571 ± 0.5 mg/g than rGO-PVA (81.0 mg/g) according to the Langmuir isotherm model. The GO-PVA foam followed electrostatic type adsorption interaction for the MB dye, while the rGO-PVA showed a π - π stacking mechanism with adsorbed MB molecules.

A biopolymer agar containing plenty of oxygen functional groups was used as reinforcing agent to prepare a GO-agar aerogel (GO-A) by mixing GO with agar suspension to obtain a hydrogel followed by freeze-drying [66]. The GO-A aerogel had an adsorption capacity of 578 mg/g for cationic MB dye. The adsorption kinetics follows the pseudo-second-order model. The adsorption mechanism was attributed to the electrostatic interactions between MB and the GO-A aerogel. Besides, the small sheets of electrospun cellulose nanofibers (CNFs) were utilized to fabricate a GO/nanofiber (G-CN) aerogel by an ice-templating freeze-dry technique to prevent over-stacking of GO sheets and to enhance connectivity of the cell walls [67]. The G-CN aerogel showed higher and selective adsorption capacity of >800 mg/g toward cationic dyes such as crystal violet (CV), methylene green, MB, or RhB in water solutions. However, the G-CN aerogel showed an insufficient adsorption performance for the removal of the anionic indigo carmine (IC) dye.

Three-dimensional printing is another emerging technique to design macroscopic graphene adsorbents toward dye removal applications. GO suspension is mixed with chemical additives such as a polymer and silica powder to obtain a highly viscous 3D printing ink [73]. Finally, the printing ink flows through a nozzle under shear force and rapid pseudoplastic for dilatant recovery after deposition. For example, Xiao et al. [71] fabricated a macroscopic rGO architecture by 3D printing technique using L-cysteine as reducing agent (rGO-Cys). The 3D adsorbent was tested to remove anionic, nonionic, and cationic dyes with conjugated aromatic structure. The rGO-Cys exhibited a high adsorption capacity of 1005 ± 1 and 1301 ± 1 mg/g for the anionic indigo carmine (IC) or the cationic dye neutral red (NR), respectively. The rGO-Cys also showed excellent adsorption performance even for multiple dye contaminations (>3500 mg/g). The π - π stacking adsorption mechanism was proposed for the high removal efficiency of rGO-Cys.

To summarize, GO sponge or graphene adsorbent foams prepared by template-directed protocols showed a high adsorption capacity to remove organic pollutants from water. However, a microporous network of GO foams with weak connections between the GO nanosheets causes instability and release of nanosheets during pollutant removal applications. While the CVD protocols are usually associated with a complicated method, high production cost and have limited potential for an application at large scale. Using soft or hard templating generally requires high-temperature calcination or complex etching processes.

11.3.2 *Template-Free Design of Graphene Sorbents via Sol-Gel Route*

The template-free design of macroscopic graphenes is usually achieved by self-concentration of physically or chemically modified GO sheets at the liquid–solid interface (Table 11.2). These designs typically employ chemical additives as cross-linkers (e.g., acid, metal ions, small, and macromolecules) to tune the gelation properties and mechanical stability of graphene hydrogels through alteration in attractive or repulsive forces between the GO in aqueous solution (Fig. 11.3c, d) [82]. Interactive mechanisms to obtain 3D graphene hydrogel can be divided into two basic categories: weak noncovalent bonding and strong covalent bonding [36]. For example, noncovalent interactions include hydrogen bond and π - π stacking between GO and hydroxyl or oxygen-rich polymers such as PVA, polyethylene oxide (PEO), polyvinyl pyrrolidone (PVP), or hydroxyl-propyl-cellulose (HPC) [83]. Ion-induced mechanism using divalent and trivalent metal ions (Ca^{+2} , Mg^{+2} , Cu^{+2} , Pb^{+2} , Cr^{+3} , Fe^{+3}) was also proposed through coordination of metal ions and oxygen functionalities of GO (e.g., hydroxyl and carboxyl groups) [84]. Furthermore, covalent bonding mechanisms include the interactions between hydroxyl and carboxyl groups of GO and nitrogen containing organic molecules (e.g., melamine, polydimethyldiallylammonium chloride (PDDA), polyethyleneimine (PHI), cetyltrimethyl

Table 11.2 Template-free designs of graphene sorbents to remove organic pollutants from water

Adsorbent	Synthesis protocol	Major additives	Pollutant	Q (mg/g)	References
Graphene hydrogel	Sol-gel at 90 °C, 5 min	DNA	Safranin	960	[74]
GO-chitosan foam	Sol-gel and vacuum dried	Chitosan	RB5	1.0	[75]
rGO-MWCNTs aerogel	Sol-gel 12 h, critical dried	MWCNTs and Vc	MB	191	[41]
Graphene-GA aerogel	Sol-gel at 95 °C, 8 h	GA	Calcein	1226	[50]
Graphene-GA aerogel	Sol-gel at 95 °C, 8 h	GA	MO	115	[50]
GO-PEI foam	Sol-gel and freeze dry	PEI	Amaranth	>800	[51]
GO-PDA hydrogel	Sol-gel at 60 °C, 6 h	PDA	RhB	207.06	[52]
GO-PDA hydrogel	Sol-gel at 60 °C, 6 h	PDA	Nitrophenol	324.89	[52]
GO-chitosan hydrogel	Sol-gel and freeze dry	Chitosan	MB and EY	>300	[53]
GO/G/PVA aerogel	Sol-gel for 12 h	PVA & glutaraldehyde	Oil	118	[54]
N and S doped rGO	Sol-gel at 90 °C, 3 h	NH ₃ H ₂ O & glutathione	MG	738.1	[62]
GO-gelatin hydrogel	Sol-gel at 95 °C	Gelatin	RhB	280	[26]
Graphene-PVA aerogel	Sol-gel and freeze dry	PVA & LC	Ionic dyes	–	[59]
PEI graphene aerogel	Sol-gel at 90 °C, 24 h	PEI	Amaranth	2043	[60]
PEI graphene aerogel	Sol-gel at 90 °C, 24 h	PEI	MO	331	[61]
Graphene-CA aerogel	Sol-gel at 90 °C	Cysteamine	MB	207.8	[15]
Graphene foam	Hydrothermal 180 °C, 12 h	Additive free	MB	215.35	[55]
Graphene foam	Hydrothermal 180 °C, 12 h	Additive free	CV	462	[56]
Spongy graphene	Hydrothermal 180 °C, 24 h	NH ₃ ·H ₂ O/NaOH	Oil	–	[76]
Graphene sponge	Hydrothermal 180 °C, 5 h	Thiourea	RhB	72.5	[38]
Graphene monolith	Hydrothermal 180 °C, 5 h	Urea	MB	50.76	[35]
Graphene monolith	Hydrothermal 95 °C, 5 h	Divalent ions & PVA	Oil	–	[77]

(continued)

Table 11.2 (continued)

Adsorbent	Synthesis protocol	Major additives	Pollutant	Q (mg/g)	References
Graphene monolith	Hydrothermal treatment	Sodium ascorbate	Bisphenol	204	[63]
rGO/CNTs aerogel	Solvothermal 200 °C, 6 h	CNTs and ethanol	MB	81.97	[78]
rGO/CNTs aerogel	Hydrothermal 120 °C, 12 h	CNT, PVP, EDTA	Oil	270	[79]
Graphene/ α -FOOH	Hydrothermal 95 °C, 5 h	Ferrous ions	Oil	–	[80]
rGO-MOF monolith	Hydrothermal 180 °C, 24 h	ZIF-67 and NH ₃ ·H ₂ O	CV	1714.2	[56]
rGO-CNFs monolith	Hydrothermal 180 °C, 5 h	TEMPO-CNFs & urea	MB	227.27	[81]

ammonium bromide (CTAB), tetramethylammonium chloride (TMAC) [82]) or biomolecules, DNA [58], and hemoglobin [85].

Physically cross-linked 3D hydrogels of GO also demonstrate through an additive-free ultra-sonication technique to convert aqueous dispersions of GO into 3D hydrogels (Fig. 11.3a, b) [16]. In this process, sonication fractures the GO nanosheets into freshly exposed smaller fragment sheet edges, which do not possess the carboxylic functional groups. Those groups are known to stabilize the GO sheets in solution (i.e., reduced repulsion force between GO sheets). It was proposed that this nonchemical induced change in surface chemistry of GO leads to a gelation of a cross-linked 3D hydrogel [16]. As-prepared hydrogels exhibit exceptionally low critical gelation concentrations ranging from ~ 0.05 to ~ 0.125 mg/mL and a porous network to host biomolecules as a carrier. However, mechanical properties and the highly hydrophilic nature of a GO hydrogel may cause serious recontamination of purified water after a pollutant removal application. Shi et al. [58] prepared graphene hydrogel by heating GO suspension and DNA at 90 °C for 5 min and tested it for the first time to remove a cationic organic dye, safranin, from water (Fig. 11.3e–g). The authors suggested that the GO/DNA hydrogel can withstand various harsh environments (e.g., acidic, alkaline, salty, or organic solvents) due to multiple non-covalent and electrostatic interactions. The hydrogel exhibited an adsorption capacity of 960 mg/g for safranin dye due to strong electrostatic attraction between the cationic dye and the negatively charged GO/DNA. Furthermore, a large surface area and porous structure were proposed to facilitate the diffusion and to increase adsorption affinity of dye molecules on the hydrogel [58].

A composite foam of chitosan and GO (GO-CS) with 3D-mesostructure was fabricated by heating a sol-mixture at 150 °C under Ar atmosphere [75]. The GO-CS foam was examined for the removal of 1 mg/L reactive black 5 (RB5) from water. The interactions of electrostatic, hydrogen bonding and van der Waals interactions between the rGO-CS and RB5 molecules were proposed to be responsible for the efficient removal of RB5 (97.5%). In another study, a hybrid aerogel of MWCNTs

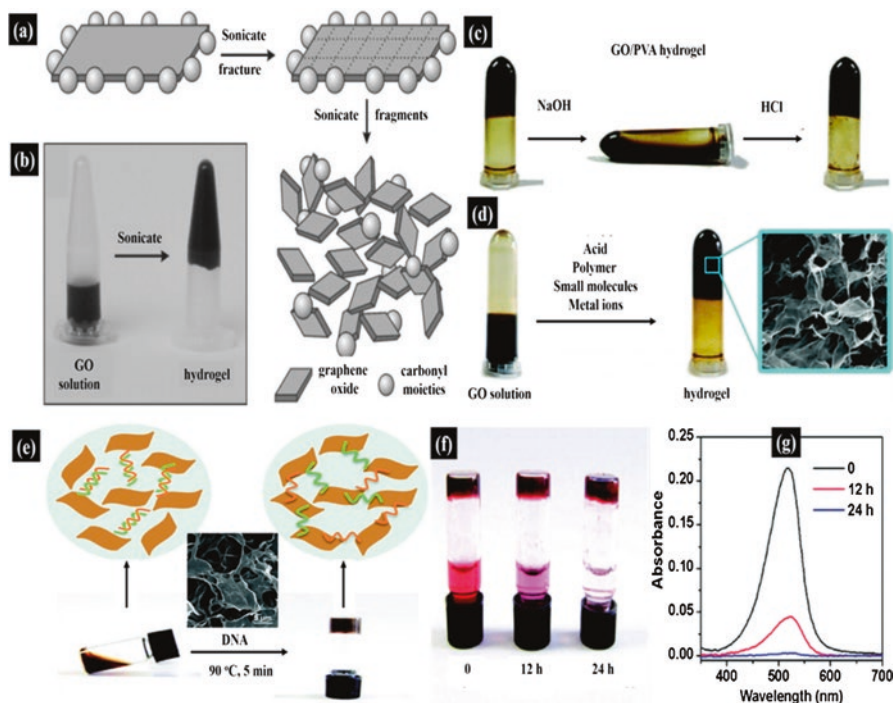


Fig. 11.3 Schematic (a) and optical images (b) of sonication assisted physically cross-linked GO hydrogel. Reproduced with permission from [16]. Copyright 2012, Elsevier. Sol-gel transition routes of chemically cross-linked graphene hydrogel using PVA (c). Acid, polymers, small molecules, and metal ions (d). Reproduced with permission from [82]. Copyright 2011, American Chemical Society. Formation of rapid GO hydrogel using single strain DNA, and inset SEM image showing 3D morphology (e), time resolved digital (f) and UV spectra of dye safranin removal (g) using GO/DNA hydrogel. Reproduced with permission from [58]. Copyright 2010, American Chemical Society

and graphene was prepared via a sol-gel protocol using vitamin C (Vc) as a reducing agent [41]. The mechanically robust hydrogel was obtained after gelation for 12 h followed by treatment with supercritical CO_2 . The graphene-MWCNTs aerogel possessed a surface area of $435 \text{ m}^2/\text{g}$ and a pore volume of $2.58 \text{ cm}^3/\text{g}$. It demonstrated a decent sorption capacity of 191 mg/g MB, 180.8 mg/g fuchsine, 150.2 mg/g RhB, and 35.8 mg/g acid fuchsine. The electrostatic interactions between oxygen functionalities of the hybrid aerogel and basic dyes was responsible for such excellent performance, while a removal of an acidic dye was associated to π - π interactions. However, the use of supercritical CO_2 drying limits the upscaling of this design to some extent. The use of different natural phenolic acids (e.g., mono-, di-, and tri-hydroxy gallic acids, GA) as reducing agents to synthesize monolithic graphene hydrogel was also demonstrated by a sol-gel method [50].

Polyethylenimine (PEI) is another effective cross-linker to prepare a self-assembled GO-PEI 3D foam by sol-gel and freeze-drying protocols. The as-obtained

GO-PEI foam showed hierarchical morphology and large specific surface area ($476 \text{ m}^2/\text{g}$) [51]. Two acidic dyes (amaranth and orange G) and one basic dye (RhB) were tested for adsorption performance. Owing to its pore-rich and amine-rich structure, the GO-PEI foam showed excellent adsorption performance for the amaranth dye (800 mg/g). In addition, polydopamine (PDA) could be used to prepare a PDA-modified graphene hydrogel (PDA-GH) via heating of a PDA and GO (2.0 mg/mL) mixture [52]. The spontaneous polymerization of dopamine was proposed for the formation of graphene hydrogel structures. The PDA-GH hydrogel was tested to remove RhB dye from water. The PDA-GH showed a maximum adsorption capacity of 207.06 mg/g for RhB, higher than that of the physically cross-linked graphene hydrogel. The chemical structure of RhB with cationic atoms (N^+) was found favorable for their adsorption on PDA-GH through electrostatic interactions. Macroscopic hydrogels of GO-CS could also be prepared using chitosan (CS) [53], PVA [54], or cysteamine (CA) [15] as cross-linker.

Generally speaking, an application of graphene in hydrogel forms usually requires complex handling processes due to high water absorption, density, and poor mechanical properties. Furthermore, large pore dimensions and complicated recollections using post-filtration in water flow-through systems call for a more rational design with robust stability and tunable porosity for water purification applications.

11.3.3 Template-Free Design of Graphene Sorbents via a Hydrothermal Pathway

A monolithic network produced by a hydrothermal reduction of GO is another alternative to create cross-linking sites between graphene sheets (Table 11.2). Xu et al. [74] developed a bottom-up synthesis to fabricate a physically cross-linked rGO hydrogel by a one-step hydrothermal method. The formation of a monolithic graphene was driven by the π - π stacking interactions between graphene sheets. It was proposed that these physical cross-linking sites were largely dependent on the GO concentration and reaction time (Fig. 11.4). For example, a GO concentration of 2 mg/mL can produce a cylindrical 3D monolith type as compared to 0.5 mg/mL GO suspension due to abundant cross-linking sites. Physically cross-linked graphene foams (GFs) can also be prepared using different lateral dimensions of GO sheets by a hydrothermal treatment at $180 \text{ }^\circ\text{C}$ for 12 h with a subsequent freeze-drying [55]. The pore dimensions of GFs using different sheet sizes of GO were ranked as: small sheet < medium sheet < large sheet. Consequently, the as-fabricated GFs showed an MB adsorption performance in the order of 215.35 mg/g (small pore size, S-GF) > 175.10 mg/g (medium pore size, M-GF) > 90.70 mg/g (large pore size, L-GF). The MB molecules strongly adhered to the GF walls via electrostatic attraction and π - π interaction.

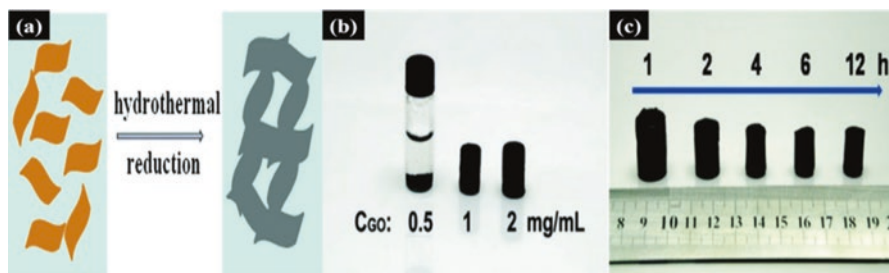


Fig. 11.4 Schematic illustration of a self-assembled graphene hydrogel (SGH) by an additive-free hydrothermal reduction (a), optical images of SGH of different concentrations at 180 °C for 12 h (b) and the products prepared with 2 mg/mL GO at 180 °C for different heating times. Reproduced with permission from [74]. Copyright 2010, American Chemical Society

Generally, the additive-free macroscopic adsorbent usually leads to poor structural strength due to loss of hydrogen bonding (i.e., physically cross-linked sites) [76] and expansion of ice crystals upon direct heat or freeze-drying [35, 38]. Alternatively, various chemical additives have been tested (e.g., ammonia solution [76], heteroatoms [35, 38], metal ions [77, 80], CNTs [41, 78, 79], polymers [86], or metal organic frameworks (MOF) [9, 56]) as cross-linkers or dopants to improve the mechanical and surface properties of 3D graphene adsorbents. For example, Yang et al. [56] prepared a monolithic rGO hydrogel by hydrothermal treatment of a GO suspension with ammonia solution ($\text{NH}_3 \cdot \text{H}_2\text{O}$, 25–28 w/w %). The removal of hydrophilic groups ($-\text{OH}$, $-\text{COOH}$, etc.) from the GO surface and a π - π stacking mechanism were proposed for the formation of the rGO hydrogel. This hydrogel showed an adsorption capacity of 462 ± 0.2 and 119 ± 0.3 mg/g for CV and MO, respectively.

Other chemical reduction routes for macroscopic rGO include the use of NaHSO_3 , Na_2S , or hydroquinone during the hydrothermal process [56]. However, the use of expensive or toxic reducing agents not only increases the cost, but also requires prolonged purification time (i.e., dialysis) to remove excess reducing agent and absorbed water during freeze-drying. Alternatively, the use of affordable and nontoxic additives (e.g., urea [35] and thiourea [38], divalent ions [77], vitamin C (Vc) or sodium ascorbate (Vc Na) [63]) as cross-linkers also yields macroscopic graphene. For example, Zhao et al. [38] used thiourea as cross-linker and reducing agent to design graphene sponge (GS). The GSs showed a tunable porous structure and surface properties with enhanced mechanical strength (140 kPa at a strain of 82%). The GS was applied to remove MB, RhB, and MO dye pollutants from water with specific sorption capacities of 184, 72.5, and 11.5 mg/g, respectively. The variability in the adsorption capacity was attributed to surface charge concentration (i.e., electrostatic interaction) and specific surface area of graphene sponges [38]. Regeneration of GS using different alcohols (methanol or ethanol) showed poor desorption performance for MB, but was suitable for desorption of RhB and MO dye. In addition, the use of divalent ions (Ca^{2+} , Ni^{2+} , or Co^{2+}) as cross-linker and/or reducing agent allowed to fabricate a self-standing graphene monoliths by

hydrothermal treatment [77]. In this case, the 3D monolith was further immersed into a PVA solution before freeze-drying in order to strengthen the mechanical properties of the monolithic graphene aerogel.

Generally speaking, the mechanical strength and dye removal performance of monolithic graphene preparations prepared through a hydrothermal method are not satisfying due to large pore dimensions in a few hundred to micrometer range sizes. Furthermore, macroscopic 3D graphene designs usually produce reduced GO of hydrophobic nature. The reduction of oxygen-containing functions from GO sheets will result in a decreased mass transfer of water-soluble dyes and an insufficient adsorption capacity. Given that, more efforts have been made to enhance the surface and mechanical properties of existing monolithic graphene adsorbents using chemical dopants.

The chemical doping using other carbonaceous nanomaterial such as single- or multi-walled CNTs is an effective approach to assemble 3D graphene composite adsorbents with superior mechanical, pore morphologies and chemical properties [41]. The hydroxyl groups of oxidized CNTs can act as hydrogen-bonding acceptor associated with oxygen functionalities of GO [78]. Furthermore, CNTs doping also enlarged the interlayer space between GO sheets [41, 79]. For instance, Ai and Jiang [78] fabricated a hybrid monolith of graphene-CNTs (G-CNTs) by a solvothermal method using a mixture of ethanol and water at 200 °C for 6 h. The reduction of oxygen-containing functional groups and self-induced π - π interactions was proposed for the random stacking interactions between graphene and CNTs to form self-assembled monoliths. The G-CNTs monolith showed an adsorption capacity of 82 ± 0.3 mg/g for the cationic MB dye than CNTs (46.2 mg/g) [87], exfoliated GO (17.3 mg/g) [34], and granular activated carbon (21.5 mg/g) [88]. The adsorption kinetics was in accordance with a pseudo-second-order kinetic model, and a Freundlich adsorption isotherm was applicable to the adsorption process.

Further efforts involve decoration with hydrophilic and affordable chemical additives such as metal organic frameworks (MOF) [9, 56], polymers (PVA) [86], or TEMPO-oxidized cellulose nanofibers (CNFs) [81] to improve the mechanical and adsorptive performance of 3D graphene adsorbents. For example, an rGO/PVA composite aerogel was fabricated by a hydrothermal and template technique [86]. The rGO/PVA aerogel had a good adsorption performance toward a wide range of dyes including cationic (i.e., RB, CV, MG, and MB), anionic (i.e., EY, AF, MO, and AB), and nonionic dyes (OR) as well as aromatic drugs (i.e., PV and TC). The π - π interaction was proposed to be the major adsorption mechanism. The removal of those compounds by the rGO-PVA aerogel was independent of dyes charge properties.

Meanwhile, the graphene materials may also serve as support to host other functional materials, which may endow the sorbents additional oxidative capabilities. For example, the loading of nanoscale TiO₂ onto macroscopic rGO has been proposed to serve as dual-functional materials for simultaneous adsorption and photocatalytic oxidation of organic pollutants from solution [13, 89]. Such design has proven to be effective for the degradation of various dyes (e.g., MB, MO, RhB, Congo red (CR), safranin, eosin Y (EY), and Azure B) from water [89]. It is worth

mentioning that the potential release of metal ions in the course of the reaction may be of concern from environmental perspective. This needs to be taken into consideration to avoid secondary pollution. Moreover, if combining with other nanoscale photocatalysts, the potential coverage of the incident light by the graphene sheets seems inevitable. This may deteriorate the overall photocatalytic oxidation performance. The integration of graphene with other advanced oxidation processes (AOPs) may be promising, since the dye molecules adsorb the incident light significantly. The integration of other processes like Fenton-like reactions or persulfate-based oxidation processes would avoid the shortcoming caused by light adsorption. These aspects should be considered, if designing other advanced dual-functional systems.

11.4 Outlook and Summary

Currently, several companies are investing in the diverse applications of graphene such as energy storage or wastewater treatment. Owing to the progress in mass production technology, the costs for graphene and derivatives have decreased significantly over the past decade. Though numerous studies suggested graphene-based materials as promising adsorbent materials, their environmental applications still face several challenges that need to be resolved further.

Firstly, the physicochemical properties of functional materials are dictated by their microstructure. GO, for example, has a highly hydrophilic nature and its nanoscale dimension make it inconvenient for practical applications. Certain GO synthesis protocols still include toxic solvents, which need to be minimized. Furthermore, most of the reports were conducted only under laboratory conditions or at bench scale. Their applications were rather limited mainly to the removal of one or a few dyes from synthetic wastewater. Such reported superior performance may fail under real conditions for the treatment of industrial dyeing wastewater with complex compositions. Moreover, the presence of large amounts of salts may significantly deteriorate or impact the overall efficiency.

Secondly, the structural integrity of a macroscopic 3D hydrogel or aerogel prepared by sol-gel route is still insufficient for flow-through systems. Harsh operating conditions (e.g., high temperature, calcination, or chemical etching), expensive chemical additives, or complex formation strategies have been observed in several cases. Development of mechanically robust 3D graphene aerogels, fine-tuning their surface functional groups and compositions, and exploring their sorption capacity and kinetics deserve further investigations. Further systematic studies on the stability, fate, and life cycle analysis of graphene-based materials cannot be overlooked and should constitute the subject of future work. In addition, mechanic and theoretical approaches will provide new insight and understanding on the rational design of advanced graphene-based sorbents for practical applications. This chapter may help to improve the knowledge of a next-generation water remediation technology based

on graphene materials and may provide the *know-how* of the rational design of functional sorbents for environmental applications.

Acknowledgments This work was supported by the Iron and Steel Joint Research Fund of National Natural Science Foundation-China BaoWu Steel Group Co., Ltd. (No. U1660107), and Specialized research fund for the Doctoral Program of Senior Education in China (Grant No. 20130075110006).

References

1. F.L. Chen, J.X. Zhu, Y.D. Yang, L.L. Wang, Assessing environmental impact of textile production with water alkalization footprint. *Sci. Total Environ.* **719**, 137522–137524 (2020)
2. X. Gang, Q. Wang, Y.J. Qian, P. Gao, Y.M. Su, Z.H. Liu, H. Chen, X. Li, J.B. Chen, Simultaneous removal of aniline, antimony and chromium by ZVI coupled with H_2O_2 : implication for textile wastewater treatment. *J. Hazard. Mater.* **368**, 840–848 (2019)
3. G. Asgari, A. Shabanloo, M. Salari, F. Eslami, Sonophotocatalytic treatment of AB113 dye and real textile wastewater using ZnO/persulfate: modeling by response surface methodology and artificial neural network. *Environ. Res.* **184**, 109367–109384 (2020)
4. C. Li, H.Y. Ma, S. Venkateswaran, B.S. Hsiao, Highly efficient and sustainable carboxylated cellulose filters for removal of cationic dyes/heavy metals ions. *Chem. Eng. J.* **389**, 123458–123470 (2020)
5. J.M.S. Oliveira, M. Silva, C.G. Issa, J.J. Corbi, M. Damianovic, E. Foresti, Intermittent aeration strategy for azo dye biodegradation: a suitable alternative to conventional biological treatments? *J. Hazard. Mater.* **385**, 121558–121565 (2020)
6. F. Teng, Z.L. Liu, A. Zhang, M. Li, Photocatalytic performances of Ag_3PO_4 polyopods for degradation of dye pollutant under natural indoor weak light irradiation. *Environ. Sci. Technol.* **49**, 9489–9494 (2015)
7. K. El Hassani, D. Kalnina, M. Turks, B.H. Beakou, A. Anouar, Enhanced degradation of an azo dye by catalytic ozonation over Ni-containing layered double hydroxide nanocatalyst. *Sep. Purif. Technol.* **210**, 764–774 (2019)
8. A. Hussain, Y. Liu, T. Bin-aftab, D. Li, W. Sand, Engineering reusable sponge of cobalt heterostructures for highly efficient organic pollutants degradation via peroxymonosulfate activation. *Chem. Nano. Mat.* **5**, 547–557 (2019)
9. W. Cheng, X.L. Lu, M. Kaneda, W. Zhang, R. Bernstein, J. Ma, M. Elimelech, Graphene oxide-functionalized membranes: the importance of nanosheet surface exposure for biofouling resistance. *Environ. Sci. Technol.* **54**, 517–526 (2020)
10. A.A. Alqadami, M. Naushad, Z.A. Alotthman, T. Ahamad, Adsorptive performance of MOF nanocomposite for methylene blue and malachite green dyes: kinetics, isotherm and mechanism. *J. Environ. Manag.* **233**, 29–36 (2018)
11. H.Q. Zhao, Y. Cheng, H.L. Lv, G.B. Ji, Y.W. Du, A novel hierarchically porous magnetic carbon derived from biomass for strong lightweight microwave absorption. *Carbon* **142**, 245–253 (2019)
12. J. Ma, Y.R. Sun, M.Z. Zhang, M.X. Yang, X. Gong, F. Yu, J. Zheng, Comparative study of graphene hydrogels and aerogels reveals the important role of buried water in pollutant adsorption. *Environ. Sci. Technol.* **51**, 12283–12292 (2017)
13. Y. Zhang, W.Q. Cui, W.J. An, L. Liu, Y.H. Liang, Y.F. Zhu, Combination of photoelectrocatalysis and adsorption for removal of bisphenol A over TiO_2 -graphene hydrogel with 3D network structure. *Appl. Catal. B Environ.* **221**, 36–46 (2018)
14. P.P. Brisebois, M. Siaz, Harvesting graphene oxide-years 1859 to 2019: a review of its structure, synthesis, properties and exfoliation. *J. Mater. Chem. C* **8**, 1517–1547 (2020)

15. C. Chen, X.Y. Zhu, B.L. Chen, Covalently cross-linked graphene oxide aerogel with stable structure for high-efficiency water purification. *Chem. Eng. J.* **354**, 896–904 (2018)
16. O.C. Compton, Z. An, K.W. Putz, B.J. Hong, B.G. Hauser, L.C. Brinson, S.T. Nguyen, Additive-free hydrogelation of graphene oxide by ultrasonication. *Carbon* **50**, 3399–3406 (2012)
17. D.R. Dreyer, S. Park, C.W. Bielawski, R.S. Ruoff, The chemistry of graphene oxide. *Chem. Soc. Rev.* **39**, 228–240 (2010)
18. U. Hofmann, R. Holst, Über die Säurenatur und die methylierung von graphitoxyd. *Ber. Dtsch. Chem. Ges.* **72**, 754–771 (1939)
19. G. Ruess, Über das graphitoxhydroxyd (graphitoxyd). *Monatsh. Chem. Verw. Teile. Anderer. Wiss.* **76**, 381–417 (1947)
20. W. Scholz, H.P. Boehm, Untersuchungen am Graphitoxid VI. Betrachtungen zur struktur des graphitoxids. *Z. Anorg. Allg. Chem.* **369**, 327–340 (1969)
21. T. Nakajima, A. Mabuchi, R.A. Hagiwara, New structure model of graphite oxide. *Carbon* **26**, 357–361 (1988)
22. A. Lerf, H. He, T. Riedl, M. Forster, J. Klinowski, ¹³C and ¹H MAS NMR studies of graphite oxide and its chemically modified derivatives. *Solid State Ionics* **101-103**, 857–862 (1997)
23. A. Lerf, H. He, M. Forster, J. Klinowski, Structure of graphite oxide revisited. *J. Phys. Chem. B* **102**, 4477–4482 (1998)
24. T. Szabó, Evolution of surface functional groups in a series of progressively oxidized graphite oxides. *Chem. Mater.* **18**, 2740–2749 (2006)
25. T.T. Ma, P.R. Chang, P.W. Zheng, F. Zhao, X.F. Ma, Fabrication of ultra-light graphene-based gels and their adsorption of methylene blue. *Chem. Eng. J.* **240**, 595–600 (2014)
26. C.Y. Liu, H.Y. Liu, A.R. Xu, K.Y. Tang, Y. Huang, C. Lu, In situ reduced and assembled three-dimensional graphene aerogel for efficient dye removal. *J. Alloys Compd.* **714**, 522–529 (2017)
27. C. Li, G. Shi, Three-dimensional graphene architectures. *Nanoscale* **4**, 5549–5563 (2012)
28. D. Krishnan, F. Kim, J.Y. Luo, R. Cruz-Silva, L.J. Cote, H.D. Jang, J.X. Huang, Energetic graphene oxide: challenges and opportunities. *Nano Today* **7**, 137–152 (2012)
29. J.J. Shao, W. Lv, Q.H. Yang, Self-assembly of graphene oxide at interfaces. *Adv. Mater.* **26**, 5586–5612 (2014)
30. S.T. Yang, S. Chen, Y. Chang, A. Cao, Y. Liu, H. Wang, Removal of methylene blue from aqueous solution by graphene oxide. *J. Colloid Interface Sci.* **359**, 24–29 (2011)
31. Y. Li, Q. Du, T. Liu, X. Peng, J. Wang, J. Sun, Comparative study of methylene blue dye adsorption onto activated carbon, graphene oxide, and carbon nanotubes. *Chem. Eng. Res. Des.* **91**, 361–368 (2013)
32. H. Yan, X. Tao, Z. Yang, K. Li, H. Yang, A.M. Li, R.S. Cheng, Effects of the oxidation degree of graphene oxide on the adsorption of methylene blue. *J. Hazard. Mater.* **268**, 191–198 (2014)
33. W. Konicki, M. Aleksandrak, D. Moszynski, E. Mijowska, Adsorption of anionic azo-dyes from aqueous solutions onto graphene oxide: equilibrium, kinetic and thermodynamic studies. *J. Colloid Interface Sci.* **496**, 188–200 (2017)
34. G.K. Ramesha, A.V. Kumara, H.B. Muralidhara, S. Sampath, Graphene and graphene oxide as effective adsorbents toward anionic and cationic dyes. *J. Colloid Interface Sci.* **361**, 270–277 (2011)
35. A. Hussain, T.B. Aftab, G. Qihao, J. Li, D. Li, The adsorptive potential of graphene monolith for organic pollutant treatment: kinetics, isotherms, and thermodynamics of interactions. *Desalin. Water Treat.* **139**, 156–165 (2019)
36. H.P. Cong, J.F. Chen, S.H. Yu, Graphene-based macroscopic assemblies and architectures: an emerging material system. *Chem. Soc. Rev.* **43**, 7295–7325 (2014)
37. K.S. Novoselov, A.K. Geim, S.V. Morozov, D. Jiang, Y. Zhang, S.V. Dubonos, I.V. Grigorieva, A.A. Firsov, Electric field effect in atomically thin carbon films. *Science* **306**, 666–669 (2004)
38. J.P. Zhao, W.C. Ren, H.M. Cheng, Graphene sponge for efficient and repeatable adsorption and desorption of water contaminations. *J. Mater. Chem.* **22**, 20197–20202 (2012)

39. J.N. Tiwari, K. Mahesh, N.H. Le, K.C. Kemp, R. Timilsina, R.N. Tiwari, K.S. Kim, Reduced graphene oxide-based hydrogels for the efficient capture of dye pollutants from aqueous solutions. *Carbon* **56**, 173–182 (2013)
40. H. Kim, S.O. Kang, S. Park, H.S. Park, Adsorption isotherms and kinetics of cationic and anionic dyes on three-dimensional reduced graphene oxide macrostructure. *J. Ind. Eng. Chem.* **21**, 1191–1196 (2015)
41. Z.Y. Sui, Q.H. Meng, X.T. Zhang, R. Ma, B. Cao, Green synthesis of carbon nanotube-graphene hybrid aerogels and their use as versatile agents for water purification. *J. Mater. Chem.* **22**, 8767–8771 (2012)
42. P. Wang, M. Cao, C. Wang, Y. Ao, J. Qian, Kinetics and thermodynamics of adsorption of methylene blue by a magnetic graphene-carbon nanotube composite. *Appl. Surf. Sci.* **290**, 116–124 (2014)
43. Y. Yao, S. Miao, S. Liu, L.P. Ma, H. Sun, S. and Wang, Synthesis, characterization, and adsorption properties of magnetic Fe₃O₄@graphene nanocomposite. *Chem. Eng. J.* **184**, 326–332 (2012)
44. W. Gao, M. Majumder, L.B. Alemany, T.N. Narayanan, M.A. Ibarra, B.K. Pradhan, Engineered graphite oxide materials for application in water purification. *ACS Appl. Mater. Interfaces* **3**, 1821–1826 (2011)
45. M. Zhang, B. Gao, Y. Yao, Y. Xue, M. Inyang, Synthesis, characterization, and environmental implications of graphene-coated biochar. *Sci. Total Environ.* **435–436**, 567–572 (2012)
46. Y.R. Liu, R. Hu, Z.Q. Zhang, A facile colloidal crystal templating method to produce three-dimensional hierarchical porous graphene-Fe₃O₄ nanocomposite for the removal of dyes from aqueous solution. *J. Porous. Mater.* **26**, 271–280 (2019)
47. F. Liu, S. Chung, G. Oh, T.S. Seo, Three-dimensional graphene oxide nanostructure for fast and efficient water-soluble dye removal. *ACS Appl. Mater. Interfaces* **4**, 922–927 (2012)
48. S. Jayanthi, N.K. Eswar, S.A. Singh, K. Chatterjee, G. Madras, A.K. Sood, Macroporous three-dimensional graphene oxide foams for dye adsorption and antibacterial applications. *RSC Adv.* **6**, 1231–1242 (2016)
49. S. Zamani, N.S. Tabrizi, Removal of methylene blue from water by graphene oxide aerogel: thermodynamic, kinetic, and equilibrium modeling. *Res. Chem. Intermed.* **41**, 7945–7963 (2015)
50. J.L. Wang, Z.X. Shi, J.C. Fan, Y. Ge, J. Yin, G.X. Hu, Self-assembly of graphene into three-dimensional structures promoted by natural phenolic acids. *J. Mater. Chem.* **22**, 22459–22466 (2012)
51. Z.Y. Sui, Y. Cui, J.H. Zhu, B.H. Han, Preparation of three-dimensional graphene oxide-polyethylenimine porous materials as dye and gas adsorbents. *ACS Appl. Mater. Interfaces* **5**, 9172–9179 (2013)
52. H.C. Gao, Y.M. Sun, J.J. Zhou, R. Xu, H.W. Duan, Mussel-Inspired synthesis of polydopamine-functionalized graphene hydrogel as reusable adsorbents for water purification. *ACS Appl. Mater. Interfaces* **5**, 425–432 (2013)
53. Y.Q. Chen, L.B. Chen, H. Bai, L. Li, Graphene oxide-chitosan composite hydrogels as broad-spectrum adsorbents for water purification. *J. Mater. Chem. A* **1**, 1992–2001 (2013)
54. S.B. Ye, Y. Liu, J.C. Feng, Low-density, mechanical compressible, water-induced self-recoverable graphene aerogels for water treatment. *ACS Appl. Mater. Interfaces* **9**, 22456–22464 (2017)
55. W. Deng, Q.L. Fang, X.F. Zhou, H.L. Cao, Z.P. Liu, Hydrothermal self-assembly of graphene foams with controllable pore size. *RSC Adv.* **6**, 20843–20849 (2016)
56. Q.X. Yang, R. Lu, S.S. Ren, C.T. Chen, Z.J. Chen, X.Y. Yang, Three dimensional reduced graphene oxide/ZIF-67 aerogel: effective removal cationic and anionic dyes from water. *Chem. Eng. J.* **348**, 202–211 (2018)
57. W.F. Chen, L.F. Yan, In situ self-assembly of mild chemical reduction graphene for three-dimensional architectures. *Nanoscale* **3**, 3132–3137 (2011)

58. Y.X. Xu, Q.O. Wu, Y.Q. Sun, H. Bai, G.Q. Shi, Three-dimensional self-assembly of graphene oxide and DNA into multifunctional hydrogels. *ACS Nano* **4**, 7358–7362 (2010)
59. J.L. Xiao, W.Y. Lv, Z. Xie, Y.H. Song, Q. Zheng, L-cysteine-reduced graphene oxide/poly(vinyl alcohol) ultralight aerogel as a broad-spectrum adsorbent for anionic and cationic dyes. *J. Mater. Sci.* **52**, 5807–5821 (2017)
60. D. Shu, F. Feng, H.L. Han, Z.F. Ma, Prominent adsorption performance of amino-functionalized ultra-light graphene aerogel for methyl orange and amaranth. *Chem. Eng. J.* **324**, 1–9 (2017)
61. Q. Zhao, X.Y. Zhu, B.L. Chen, Stable graphene oxide/poly(ethyleneimine) 3D aerogel with tunable surface charge for high performance selective removal of ionic dyes from water. *Chem. Eng. J.* **334**, 1119–1127 (2018)
62. Y.C. Shi, A.J. Wang, X.L. Wu, J.R. Chen, J.J. Feng, Green-assembly of three-dimensional porous graphene hydrogels for efficient removal of organic dyes. *J. Colloid Interface Sci.* **484**, 254–262 (2016)
63. Z. Fang, Y. Hu, W. Zhang, X. Ruan, Shell-free three-dimensional graphene-based monoliths for the aqueous adsorption of organic pollutants. *Chem. Eng. J.* **316**, 24–32 (2017)
64. R.J. Zhang, Y.C. Cao, P.X. Li, X.B. Zang, P.Z. Sun, K.L. Wang, M.L. Zhong, J.Q. Wei, D.H. Wu, F.Y. Kang, H.W. Zhu, Three-dimensional porous graphene sponges assembled with the combination of surfactant and freeze-drying. *Nano Res.* **7**, 1477–1487 (2014)
65. N. Wang, P.R. Chang, P.W. Zheng, X.F. Ma, Graphene-poly(vinyl alcohol) composites: fabrication, adsorption and electrochemical properties. *Appl. Surf. Sci.* **314**, 815–821 (2014)
66. L. Chen, Y.H. Li, Q.J. Du, Z.H. Wang, Y.Z. Xia, E. Yedinak, J. Lou, L.J. Ci, High performance agar/graphene oxide composite aerogel for methylene blue removal. *Carbohydr. Polym.* **155**, 345–353 (2017)
67. J.L. Xiao, W.Y. Lv, Y.H. Song, Q. Zheng, Graphene/nanofiber aerogels: performance regulation towards multiple applications in dye adsorption and oil/water separation. *Chem. Eng. J.* **338**, 202–210 (2018)
68. H. Ha, K. Shanmuganathan, C.J. Ellison, Mechanically stable thermally cross linked poly(acrylic acid)/reduced graphene oxide aerogels. *ACS Appl. Mater. Interfaces* **7**, 6220–6229 (2015)
69. H.Y. Mi, X. Jing, A.L. Politowicz, E. Chen, H.X. Huang, L.S. Turng, Highly compressible ultra-light anisotropic cellulose/graphene aerogel fabricated by bidirectional freeze drying for selective oil absorption. *Carbon* **132**, 199–209 (2018)
70. X.C. Dong, J. Chen, Y.W. Ma, J. Wang, M.B. Chan-Park, X.M. Liu, L.H. Wang, W. Huang, P. Chen, Superhydrophobic and superoleophilic hybrid foam of graphene and carbon nanotube for selective removal of oils or organic solvents from the surface of water. *Chem. Commun.* **48**, 10660–10662 (2012)
71. J.L. Xiao, W.Y. Lv, Z. Xie, Y.Q. Tan, Y.H. Song, Q. Zheng, Environmentally friendly reduced graphene oxide as a broad-spectrum adsorbent for anionic and cationic dyes via pi-pi interactions. *J. Mater. Chem. A* **4**, 12126–12135 (2016)
72. J.L. Vickery, A.J. Patil, S. Mann, Fabrication of graphene-polymer nanocomposites with higher-order three-dimensional architectures. *Adv. Mater.* **21**, 2180–2184 (2009)
73. A.E. Jakus, E.B. Secor, A.L. Rutz, S.W. Jordan, M.C. Hersam, R.N. Shah, Three-dimensional printing of high-content graphene scaffolds for electronic and biomedical applications. *ACS Nano* **9**, 4636–4648 (2015)
74. Y.X. Xu, K.X. Sheng, C. Li, G.Q. Shi, Self-assembled graphene hydrogel via a one-step hydrothermal process. *ACS Nano* **4**, 4324–4330 (2010)
75. J.S. Cheng, J. Du, W.J. Zhu, Facile synthesis of three-dimensional chitosan-graphene meso-structures for reactive black 5 removal. *Carbohydr. Polym.* **88**, 61–67 (2012)
76. H. Bi, X. Xie, K. Yin, Y. Zhou, S. Wan, L. He, F. Xu, F. Banhart, L. Sun, R.S. Ruoff, Spongy graphene as a highly efficient and recyclable sorbent for oils and organic solvents. *Adv. Funct. Mater.* **220**, 4401–4401 (2012)

77. X. Jiang, Y.W. Ma, J.J. Li, Q.L. Fan, W. Huang, Self-assembly of reduced graphene oxide into three-dimensional architecture by divalent ion linkage. *J. Phys. Chem. C* **114**, 22462–22465 (2010)
78. L.H. Ai, J. Jiang, Removal of methylene blue from aqueous solution with self-assembled cylindrical graphene-carbon nanotube hybrid. *Chem. Eng. J.* **192**, 156–163 (2012)
79. W. Wan, R. Zhang, W. Li, H. Liu, Y. Lin, L. Li, Y. Zhou, Graphene-carbon nanotube aerogel as an ultra-light, compressible and recyclable highly efficient absorbent for oil and dyes. *Environ. Sci. Nano* **3**, 107–113 (2016)
80. H.P. Cong, X.C. Ren, P. Wang, S.H. Yu, Macroscopic multifunctional graphene-based hydrogels and aerogels by a metal ion induced self-assembly process. *ACS Nano* **6**, 2693–2703 (2012)
81. A. Hussain, J. Li, J. Wang, F. Xue, Y. Chen, T.B. Aftab, D. Li, Hybrid monolith of graphene/TEMPO-oxidized cellulose nanofiber as mechanically robust, highly functional, and recyclable adsorbent of methylene blue dye. *J. Nanomater.* **2018**, 1–12 (2018)
82. H. Bai, C. Li, X.L. Wang, G.Q. Shi, On the gelation of graphene oxide. *J. Phys. Chem. C* **115**, 5545–5551 (2011)
83. C.C. Huang, H. Bai, C. Li, G.Q. Shi, A graphene oxide/hemoglobin composite hydrogel for enzymatic catalysis in organic solvents. *Chem. Commun.* **47**, 4962–4964 (2011)
84. H. Bai, C. Li, X.L. Wang, G.Q. Shi, A pH-sensitive graphene oxide composite hydrogel. *Chem. Commun.* **46**, 2376–2378 (2010)
85. H. Bai, C. Li, G.Q. Shi, Functional composite materials based on chemically converted graphene. *Adv. Mater.* **23**, 1089–1115 (2011)
86. J.L. Xiao, J.F. Zhang, W.Y. Lv, Y.H. Song, Q. Zheng, Multifunctional graphene/poly(vinyl alcohol) aerogels: in situ hydrothermal preparation and applications in broad-spectrum adsorption for dyes and oils. *Carbon* **123**, 354–363 (2017)
87. Y.J. Yao, F.F. Xu, M. Chen, Z.X. Xu, Z.W. Zhu, Adsorption behavior of methylene blue on carbon nanotubes. *Biores. Technol.* **101**, 3040–3046 (2010)
88. J. Yener, T. Kopac, G. Dogu, T. Dogu, Dynamic analysis of sorption of Methylene Blue dye on granular and powdered activated carbon. *Chem. Eng. J.* **144**, 400–406 (2008)
89. Y. Zhao, Y. Zhang, A. Liu, Z. Wei, S. Liu, Construction of three-dimensional hemin-functionalized graphene hydrogel with high mechanical stability and adsorption capacity for enhancing photodegradation of methylene blue. *ACS Appl. Mater. Interfaces* **9**, 4006–4014 (2017)